



Open access

<https://jrisetgeotam.brin.go.id/index.php/jrisgeotam>

Research article

Landslide susceptibility zonation using weight of evidence method in Mertelu and Tegalrejo, Gedangsari, Gunungkidul, Special Region of Yogyakarta, Indonesia

Mochammad Farhan Dzaki¹, Hendy Setiawan^{1*}, Rahmadi Hidayat¹

¹Department of Geological Engineering, Faculty of Engineering, Universitas Gadjah Mada
Jalan Grafika no 2, Yogyakarta, 55281, Indonesia

Keywords:

landslide
Gedangsari
weight of evidence
susceptibility zone

Corresponding author:

Hendy Setiawan
Email address: hendy.setiawan@ugm.ac.id

Article history

Received : 04 April 2024
Revised : 03 December 2024
Accepted : 05 December 2024

©2024 The Author(s), Published by
National Research and Innovation Agency
BRIN

This is an open access article under
the CC BY-SA license
(<https://creativecommons.org/licenses/by-sa/4.0/>).



ABSTRACT

Mertelu and Tegalrejo are situated in the Gedangsari Sub-district, Gunungkidul Regency, Special Region of Yogyakarta, Indonesia. Located in the northern Baturagung Range, Southern Mountains Zone of East Java, with much hilly topography and mountainous areas with steep slopes, Mertelu and Tegalrejo are prone to landslides. The purpose of this research is to produce a landslide susceptibility zone using the weight of evidence (WoE) method. There were 73 landslide data taken from December 2022 to January 2023. As much as 80% of the data were used as a training dataset for weighting and generating the model map, while the remaining 20% were used as a test dataset. Parameters used in this research include slope angle, lithology, distance to faults, distance to rivers, and land use. Each parameter was weighted using the WoE method, and then the map of each parameter was overlaid to produce a map of landslide susceptibility zones. The accuracy of the map was calculated using the area under curve (AUC) method, including the success rate curve (SRC) and prediction rate curve (PRC). Based on the research results, the landslide susceptibility zone in the research area can be categorized: (1) very low, covering 6.34% of the total research area, (2) low, covering 24.15% of the total research area, (3) moderate, covering 44.46% of the total research area, and (4) high, covering 25.05% of the total research area. The landslide susceptibility map shows that the research location is predominantly characterized by areas with medium to high susceptibility to landslides. The medium and high susceptibility zones are close to the rivers that serve as the alignment of the faults. The accuracy calculations result in an SRC value of 0.753 and a PRC value of 0.780, both can be classified as “good” performance.

INTRODUCTION

Landslides are described as geological disasters where the slope materials in the form of soil and rock move down along the slip surface under the control of gravity due to factors that disturb the stability of the slope (Hung et al., 2014; Karnawati, 2007). The stability of a slope can be influenced by two factors, i.e., the controlling factor and the triggering factor (Karnawati, 2007). The controlling factor is a natural condition of the slope itself that renders a slope susceptible to movement, while the triggering factor is a process that causes a slope to move significantly due to the exceeding of the critical limits of the slope stability (Karnawati, 2007).

Landslides are a natural disaster that commonly occurs in Indonesia, especially in Gunungkidul Regency, Special Region of Yogyakarta. The northern part of Gunungkidul Regency is prone to landslides, for example, the Gedangsari Sub-District (PVMBG, 2013; Yatini & Suyanto, 2018). Tegalrejo and Mertelu are two of the Gedangsari Sub-District areas with high susceptibility to landslides (Budianta, 2020; PVMBG, 2013). These villages have much hilly topography and mountainous areas with steep slopes which can cause landslides. One of the landslide incidents occurred on February 16th, 2023 in Tegalrejo, Gedangsari Sub-District, Gunungkidul Regency, Special Region of Yogyakarta, which caused heavy damage to the main road that connecting two districts (Figure 1).



Figure 1 Landslide occurrence in Tegalrejo, Gedangsari on February 16th, 2023, documented during site investigation on March 4th, 2023

Considering the impact of landslides on the communities in Mertelu and Tegalrejo, a more detailed study of the landslide susceptibility mapping in this area is necessary for settlement planning and hazard mitigation. Landslide susceptibility mapping has already been developed using various weighting methods such as semi-qualitative analytical hierarchy process (AHP), qualitative heuristic approach, statistical frequency ratio (FR), and fuzzy logic (FL), both with the help of remote sensing and geographical information systems (Bacha et al., 2018; Blais-Stevens et al., 2012; Dai et al., 2001; Shirzadi

et al., 2017; van Westen et al., 2008; Yalcin & Bulut, 2007). Quantification of assigned controlling factors with possible weighting related to landslide inventory data in the landslide susceptibility mapping can be approached using bivariate statistical methods. Examples of bivariate methods that emphasize a conditional probability-based are the frequency contrast method, the information value method, the certainty factor method, and the weight of evidence method (Das et al., 2023; Li & Lan, 2023).

One of the bivariate statistical methods commonly used in landslide susceptibility is the weight of evidence (WoE) method (Dahal et al., 2008; Getachew & Meten, 2001; Ilia & Tsangaratos, 2016; Kumar & Anbalagan, 2019; Pamela et al., 2018; Pradhan et al., 2010). The WoE method is a quantitative and data-driven approach designed to produce weighted data by combining multiple data parameters. To avoid subjectivity in determining landslide susceptibility zones, the WoE method, as a data-driven approach, was utilized to produce a landslide susceptibility zoning map in Mertelu and Tegalrejo, Gedangsari sub-district, Gunungkidul Regency, Special Region of Yogyakarta.

STUDY AREA

The study area is located at Tegalrejo and Mertelu Villages, Gedangsari Sub-district, Gunungkidul Regency, Special Region of Yogyakarta, with an area of around 19.19 km² (Figure 2). According to the coordinate system, the research location is located in UTM 49S and bordered by coordinates 455681 E in the west, 9138202 N in the north, 462406 E in the east, and 9132140 N in the south. The research location is approximately 40 km to the northeast of Yogyakarta City.

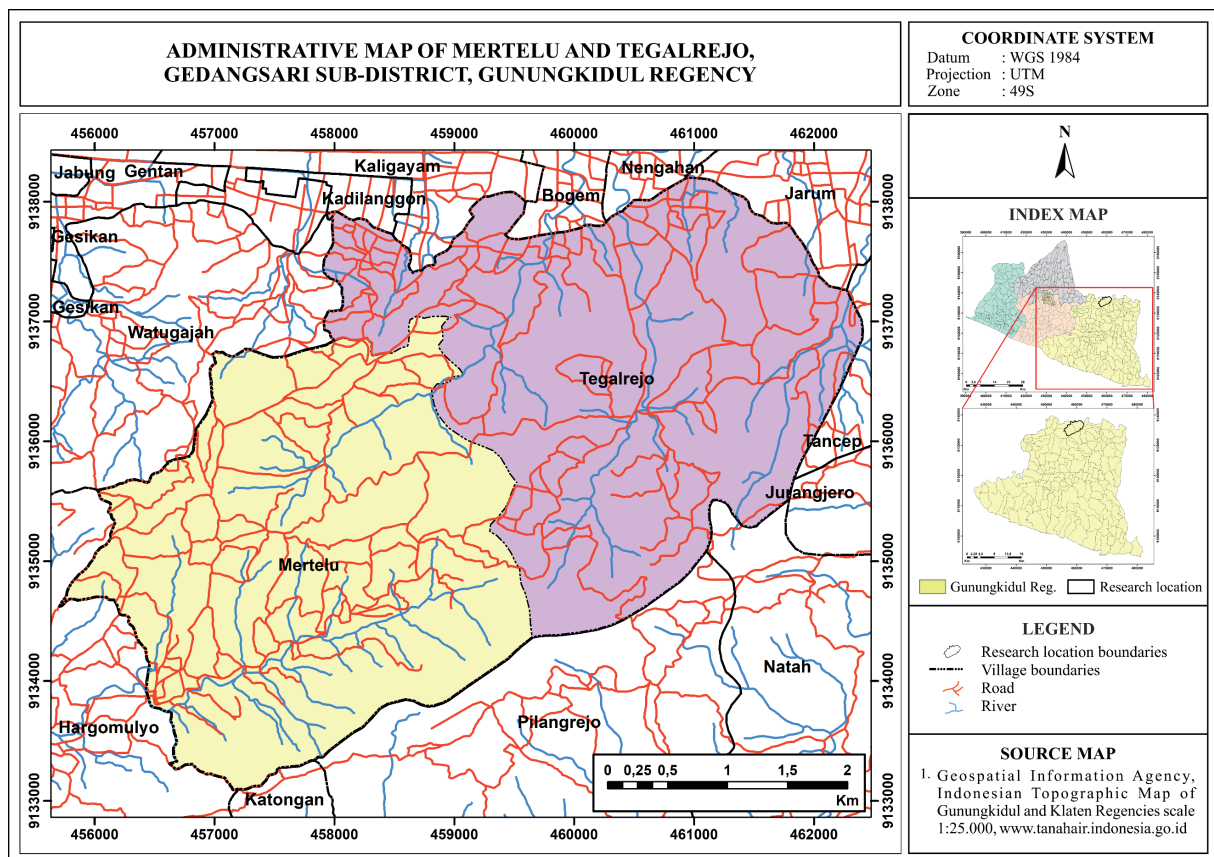


Figure 2. Research location in Mertelu and Tegalrejo, Gedangsari Sub-district, Gunungkidul Regency, Special Region of Yogyakarta

GEOLOGICAL SETTING OF MERTELU AND TEGALREJO

The research location is the northern Baturagung Range, Southern Mountains Zone of East Java (*Pegunungan Selatan Jawa Timur*). The stratigraphy in the research location consists of three formations, i.e., Kebo Formation, Butak Formation, and Semilir Formation (Barianto et al., 2017) (Figure 3). These three rock formations are composed of volcanic sedimentary rock. The Kebo Formation is composed of interbedded lithological units of volcanic breccia, sandstone, and gravelly sandstone with intercalations of siltstone, mudstone, tuff, and shale. The Butak Formation is composed of polymic breccia with intercalations of sandstone, gravelly sandstone, mudstone, siltstone, and shale. Then, the Semilir Formation is composed of tuff, pumice breccia, tuffaceous sandstone, and shale (Barianto et al., 2017).

There are two main faults at the research location, namely the Tegalrejo Fault and the Cremo Fault. The Tegalrejo Fault is a right-lateral strike-slip fault identified based on minor faults and lineaments along the Tegalrejo River. Meanwhile, the Cremo Fault is a left-lateral strike-slip fault delineated based on the alignment of the Cremo River. The Tegalrejo fault has a northwest-southeast orientation, while the Cremo fault has a southwest-northeast orientation. Both faults cut across these three rock formations in the research location (Barianto et al., 2017).

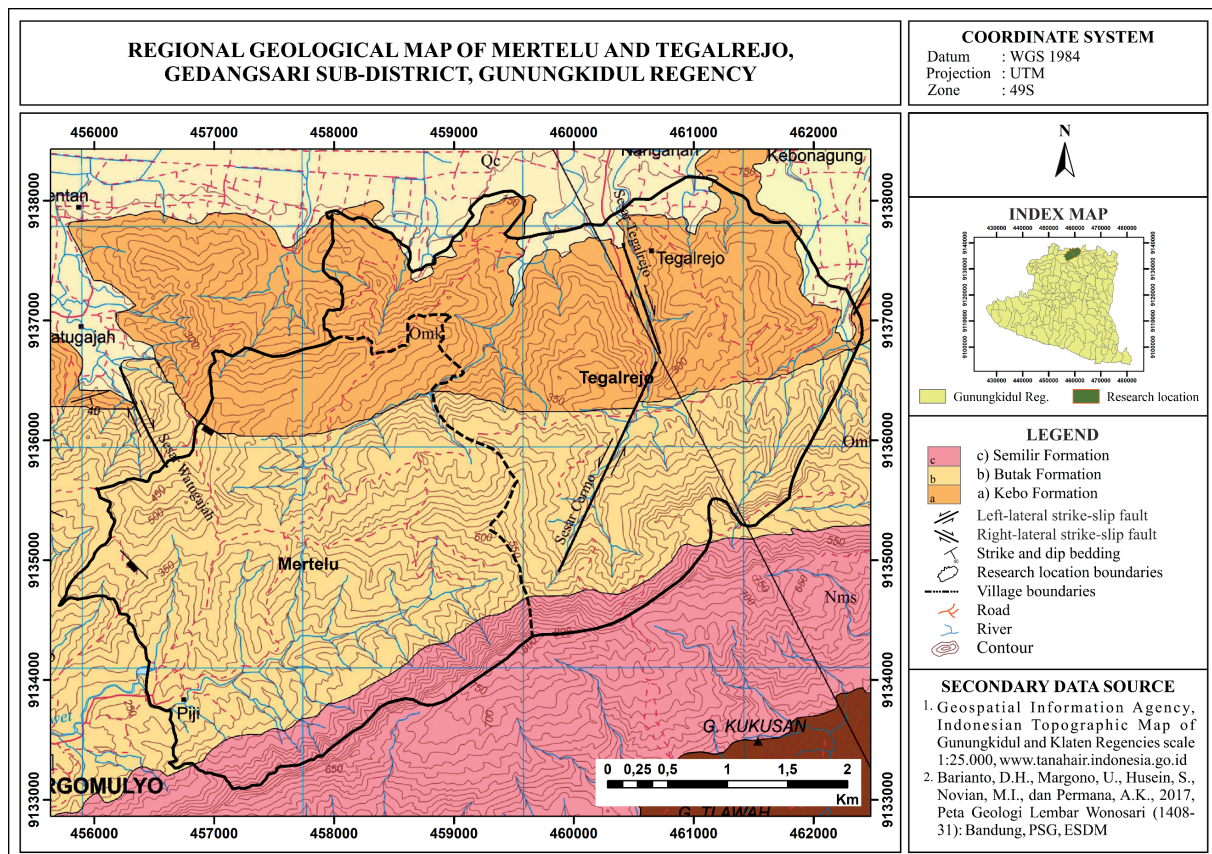


Figure 3. Regional geological map of Mertelu and Tegalrejo, Gedangsari Sub-district, Gunungkidul Regency, Special Region of Yogyakarta (Barianto et al., 2017)

METHODOLOGY

The weight of evidence (WoE) method is a quantitative and data-driven method designed to produce weighted data by combining multiple data parameters (Ilia & Tsangaratos, 2016; Kumar & Anbalagan, 2019; Pamela et al., 2018). The WoE method focuses on the comparison between the area of landslides with the area of parameters causing landslides. This comparison produces the weight values of parameters and the prediction of the areas prone to landslides. In this research, landslide controlling

factors are utilized as parameters for determining landslide susceptibility zones using the WoE method: slope angle, lithology, distance to faults, distance to rivers, and land use. In other research (e.g., Pamela et al., 2018), the parameters controlling or causing landslides are called geofactors.

The weighted system in WoE is divided into positive weight and negative weight. The positive weight (W^+) describes the weight of the probability of landslides in geofactors. Meanwhile, the negative weight (W^-) describes the weight of improbability of landslides in geofactors (Pamela et al., 2018). The formulation of WoE is written as follows:

$$W^+ = \ln \left(\frac{\left(\frac{\text{landslide area in class } (x)}{\text{total landslide area } (Z)} \right)}{\left(\frac{\text{stable area in class } (a)}{\text{total stable area } (c)} \right)} \right) \quad (1)$$

$$W^- = \ln \left(\frac{\left(\frac{\text{landslide area outside class } (y)}{\text{total landslide area } (Z)} \right)}{\left(\frac{\text{stable area outside class } (b)}{\text{total stable area } (c)} \right)} \right) \quad (2)$$

$$C_w = W^+ - W^- \quad (3)$$

Where x is the landslide area in class, z is the total landslide area, a is a stable area in class, c is the total stable area, y is the landslide area outside class, and b is a stable area outside class, and C_w is the contrast weight value.

The maps of all landslide susceptibility parameters were prepared with the value of contrast weight, which was inserted using the “Field Calculator” tool in the “Attribute Table” window of ArcMap. Then, the maps of all landslide susceptibility parameters were overlaid to generate a landslide susceptibility zone map with a landslide susceptibility index (LSI) attribute (Figure 4). LSI is the total summation of contrast weight values from all landslide susceptibility parameters. The LSI equation is shown in Equation 4.

$$LSI = C_{\text{slope angle}} + C_{\text{lithology}} + C_{\text{faults}} + C_{\text{rivers}} + C_{\text{land use}} \quad (4)$$

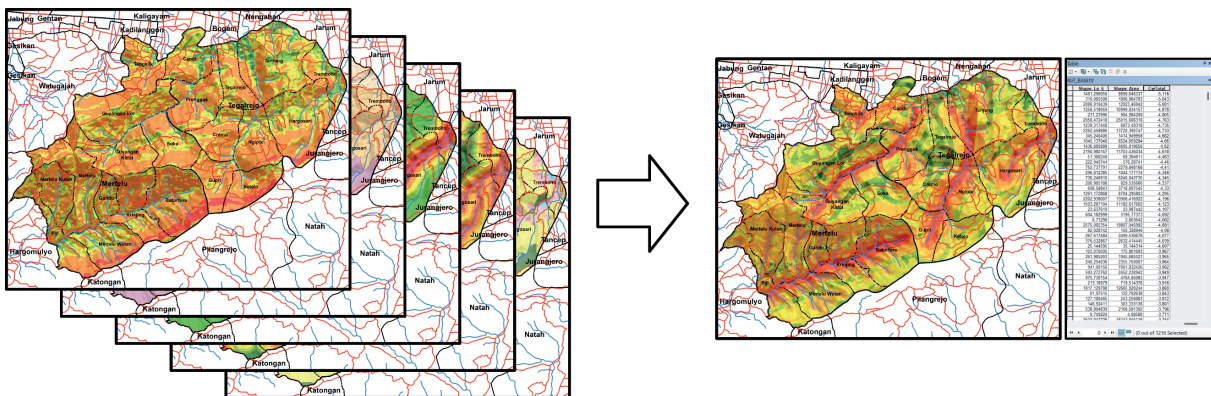


Figure 4. Illustration of overlaying landslide susceptibility parameter maps

Where $C_{\text{slope angle}}$ is the contrast weight value of the slope angle parameter, $C_{\text{lithology}}$ is the contrast weight value of the lithology parameter, C_{faults} is the contrast weight value of distance to faults parameter, C_{rivers} is the contrast weight value of distance to rivers parameter, and $C_{\text{land use}}$ is the contrast weight values of land use parameter.

The result of weighting parameters were then categorized and validated using the success rate curve (SRC) and prediction rate curve (PRC) methods (Pamela et al., 2018; Ilija & Tsangaratos, 2016; Pradhan

et al., 2010). The values of SRC and PRC are obtained by calculating the area under the curve (AUC) to check the accuracy of the map (Getachew & Meten, 2001; Pamela et al., 2018; Pradhan et al., 2010). AUC is an index value derived from a comparison graph between the percentage of the area of the parameter class versus the percentage of the area of landslides within each parameter class. A model will be classified as “fair” if the AUC value is greater than 0.6 (Table 1) (Bekkar et al., 2013).

Table 1. Classification of AUC Value (Bekkar et al., 2013)

AUC Value	Accuracy Level
0.5–0.6	Poor
0.6–0.7	Fair
0.7–0.8	Good
0.8–0.9	Very good
0.9–1.0	Excellent

RESULT AND DISCUSSION

The data used in this research are primary and secondary data. The primary data were obtained by direct observation of geological conditions and landslides from the field, including lithology, geological structure, geomorphology, landslide points, and landslide area. Meanwhile, the secondary data were obtained from previous research or related references, including the Digital Elevation Model (DEM), the Regional Geological Map of Wonosari, Gunungkidul (Barianto, et al., 2017), and the Indonesia Topographic Map of Gunungkidul and Klaten Regencies from Geospatial Information Agency (2014). The obtained data are used to determine the weighting values of each parameter required in assessing the susceptibility zone of landslides using the WoE method.

Geological condition

The geomorphological setting of the research location was classified into three geomorphological units, that is (1) unit of structural hills with a gentle slope, (2) unit of structural hills with a steep slope, and (3) unit of structural hills with a very steep slope. The classification of geomorphological units is based on morphography, morphogenesis, and morphometrics according to Van Zuidam's classification (van Zuidam, 1985) (Figure 5 and Figure 6).

The lithology in the research location is dominated by volcanic sedimentary rock and grouped into three lithological units, i.e., (1) unit of interbedded tuffaceous sandstone-siltstone with claystone intercalations, (2) unit of tuffaceous sandstone with siltstone, breccia, and tuff intercalations, and (3) unit of interbedded tuffaceous sandstone-lapilli tuff with tuff intercalations (Figure 7 and Figure 8). The lithological units (1) and (2) are similar to the Kebo-Butak Formation, while the lithological unit (3) is similar to the Semilir Formation (Surono, 2009). The research location also has seven faults, with three of them identified as normal faults, another three identified as left-lateral strike-slip faults, and the remaining one identified as right-lateral strike-slip faults. Meanwhile, based on their main orientation, two of them are classified as northwest-southeast orientation faults, while the remaining five are classified as southwest-northeast orientation faults (Figure 7). The faults with southwest-northeast orientation are classified within the Meratus structure pattern, which is Late Eocene to Middle Miocene in age. The Meratus structure pattern is the oldest structural pattern and is uniformly distributed in the Southern Mountains. Meanwhile, the faults with northwest-southeast orientation are classified within the Sumatera structure pattern, which is Late Pliocene in age (Prasetyadi et al., 2011).

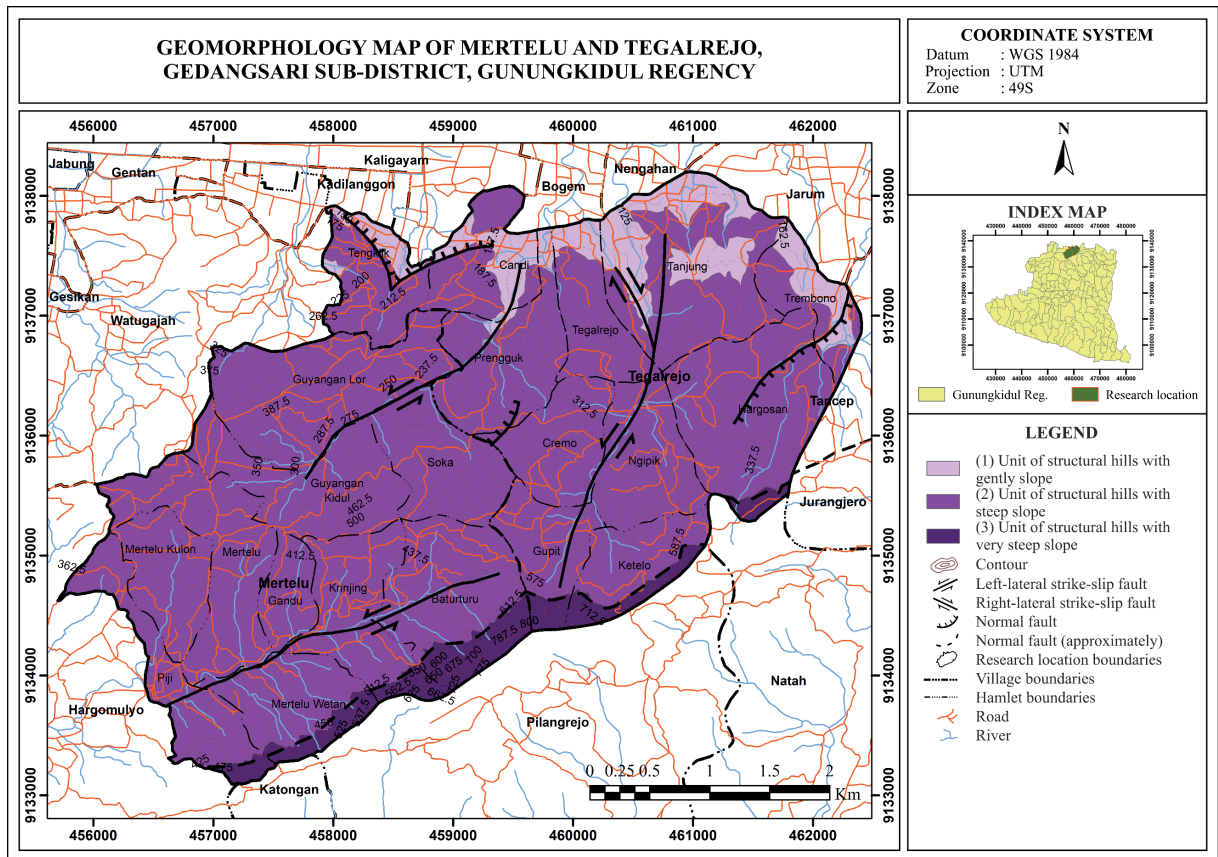


Figure 5. Geomorphological map of Mertelu and Tegalrejo

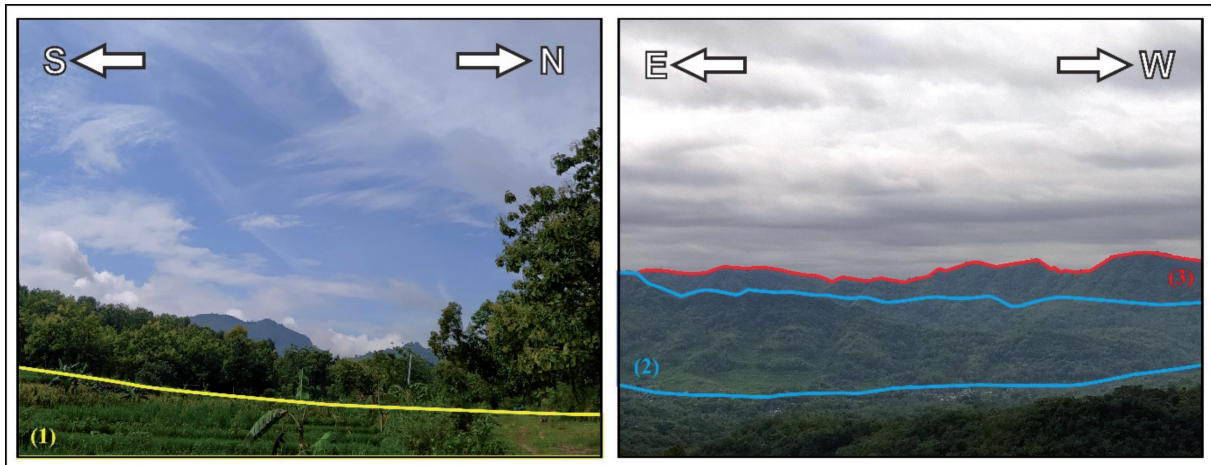


Figure 6. Documentation of geomorphological units: (1) unit of structural hills with a gentle slope (left); (2) unit of structural hills with a steep slope, and (3) unit of structural hills with a very steep slope (right)

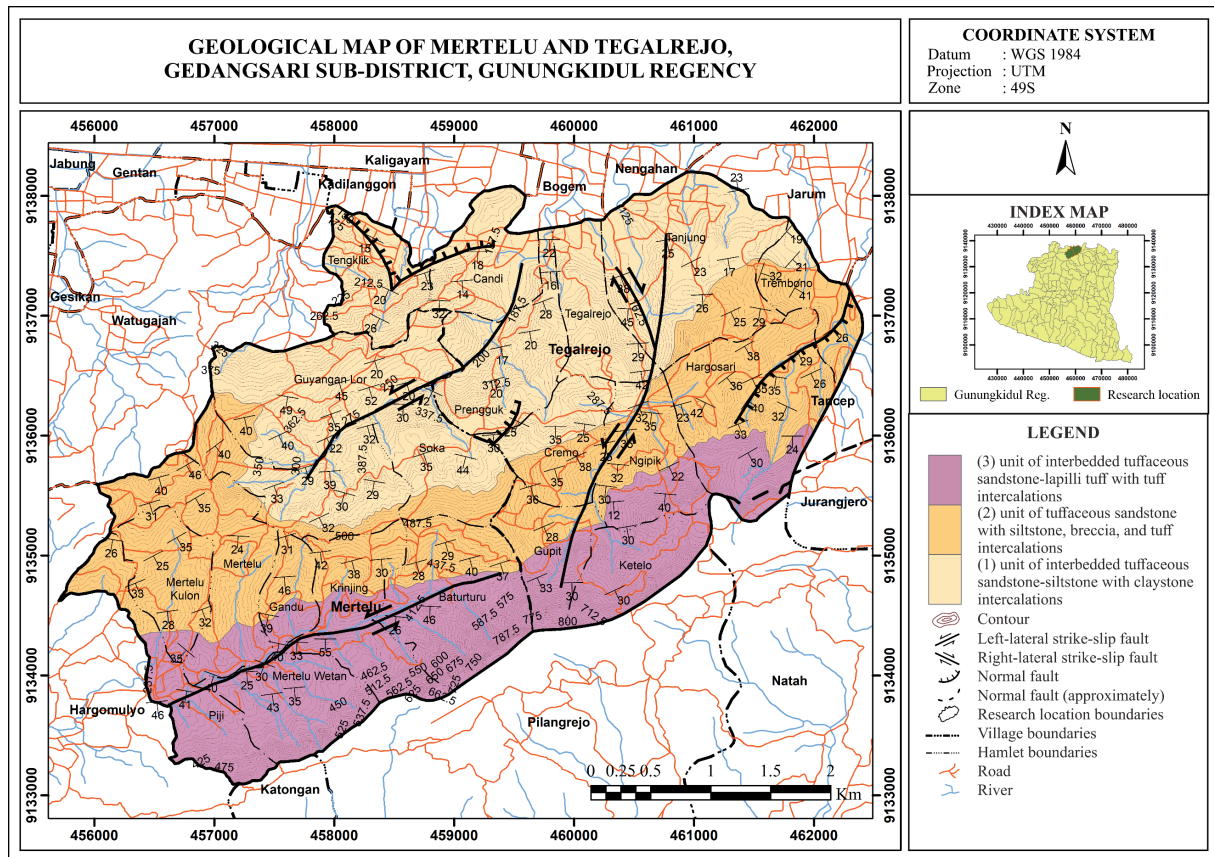


Figure 7. Geological map of Mertelu and Tegalrejo

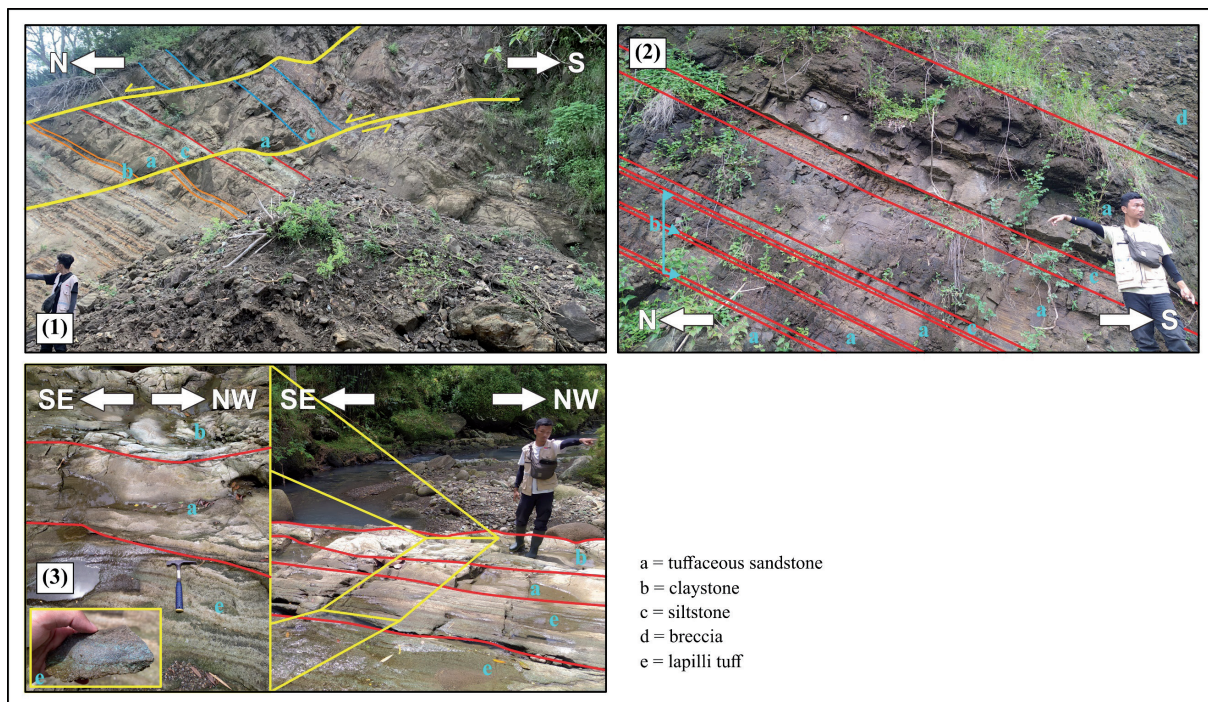


Figure 8. Documentation of geological units: (1) unit of interbedded tuffaceous sandstone-siltstone with claystone intercalations, (2) unit of tuffaceous sandstone with siltstone, breccia, and tuff intercalations, and (3) unit of interbedded tuffaceous sandstone-lapilli tuff with tuff intercalations

Landslide inventory

The WoE method requires landslide data in the form of location and area. Therefore, a total of 73 landslide locations and areas were mapped from direct observation in the field from December 2022 to January 2023 (Table 2 and Figure 10a). The landslide data obtained were divided into two datasets: the training dataset of 80% and the test dataset of 20% from the total landslide data distribution (Pradhan et al., 2010). The low percentage of the training dataset will lead to a decrease in the confidence of the weights, while the low percentage of the test dataset will keep statistical strength in the model (Getachew & Meten, 2001). In this research, the total area of landslide used for the training dataset is 6,427.25 m², while that used for the test dataset is 482.75 m², and the total area of the research location is 19,189,246.01 m² or approximately 19.19 km².

Landslide susceptibility parameters

Slope angle

The slope angle parameter represents the morphology aspect. Morphology has a significant role in the mass movement of slopes. In general, the steeper the slope, the higher the susceptibility of the slope to move. The research location, which is located in the Baturagung Range, has a much hilly and mountainous morphology with steep slopes. Therefore, the slope angle parameter is considered a controlling factor of the landslide's occurrence at the research location. The slope angle map was derived from DEMNAS and then reclassified according to Van Zuidam's slope classification (van Zuidam, 1985). The slope angle map of the research location was reclassified into five classes: 2°-4°, 4°-8°, 8°-16°, 16°-35°, and 35°-55° (Figure 10b). The distribution of landslide area showed that 67.08% of the total landslide area was concentrated in the slope angle class of 16°-35° (Figure 9), as shown in Table 2.



Figure 9. Landslide evidence in the slope angle class of 16°-35°

Lithology

The variations of lithological and structural conditions affect the compactness, strength, and permeability of rocks. Based on geological mapping, the research location has been grouped into three lithological units: (1) unit of interbedded tuffaceous sandstone-siltstone with claystone intercalations, (2) unit of tuffaceous sandstone with siltstone, breccia, and tuff intercalations, and (3) unit of interbedded tuffaceous sandstone-lapilli tuff with tuff intercalations (Figure 10c). The distribution of landslide area showed that the landslides area was concentrated in the lithological unit of tuffaceous sandstone with siltstone, breccia, and tuff intercalations, as much as 48.64% of the total landslides area, as shown in Table 2.

Table 2. Distribution of landslide in each of the class parameters

Parameters	Classes	Stable Area in Class (m ²)	Landslide Area in Class (m ²)	% Landslide Area
Slope angle	2°-4°	618,562.02	0.00	0.00
	4°-8°	1,927,434.89	0.00	0.00
	8°-16°	6,280,411.98	2,056.75	32.92
	16°-35°	9,747,955.11	4,190.50	67.08
	35°-55°	614,881.99	0.00	0.00
Lithology	(1) unit of interbedded tuffaceous sandstone-siltstone with claystone intercalations	7,733,418.93	1,599.25	25.60
	(2) unit of tuffaceous sandstone with siltstone, breccia, and tuff intercalations	6,433,835.85	3,038.75	48.64
	(3) unit of interbedded tuffaceous sandstone-lapilli tuff with tuff intercalations	5,021,991.22	1,609.25	25.76
Distance to Faults	<100 m	2,798,019.71	3,504.25	56.09
	100-200 m	2,939,007.30	1,081.50	17.31
	200-300 m	2,982,617.81	645.50	10.33
	300-400 m	2,883,527.67	84.00	1.34
	>400 m	7,586,073.52	932.00	14.92
Distance to Rivers	<50 m	4,081,002.30	2,883.75	46.16
	50-100 m	3,703,912.76	1,341.50	21.47
	100-150 m	3,128,027.60	719.25	11.51
	150-200 m	2,551,525.25	408.00	6.53
	200-250 m	2,019,182.52	454.50	7.28
	250-300 m	1,481,428.58	0.00	0.00
	>300 m	2,224,166.99	440.25	7.05
Land Use	Settlement	2,233,805.07	292.50	4.68
	Rice field	112,321.89	0.00	0.00
	Orchard	479,862.54	0.00	0.00
	Shrubland	597,427.92	141.00	2.26
	Grassland	69,926.67	0.00	0.00
	Agricultural Field	15,695,901.91	5,813.75	93.06

Distance to faults

Faults emerge in response to deformation when a rock undergoes compression and extension. Deformation in rocks leads to the weakening of bonds between particles and increases the permeability of rock. These conditions cause the area around fault lines to be in a weak zone. The fault lines in the research location were mapped based on geological observation in the field. The distance to fault zones can be derived using the “Buffer” tool into five classes: <100 m, 100-200 m, 200-300 m, 300-400 m, and >400 m (Figure 10d). The delineation of weak zones is based on the distance from the fault line. The distribution of landslide area showed that 56.09% of the total landslide area was concentrated in the distance to faults class of <100 m, as shown in Table 2.

Distance to rivers

The distance to rivers parameter represents the hydrogeological aspect of the research location. The river is considered to potentially influence the water saturation of a slope. The proximity of a slope to a river correlates with a higher water saturation level compared to a slope located farther away from the river. A saturated slope can lead the materials of the slope to reach the limits of plasticity and liquidity, thereby causing mass movement because of the changes volume of slope materials (Cellek, 2023). The river map has been obtained from the Indonesia Topographic Map of the research location. The distance to a river can be derived using the “Buffer” tool into seven classes: <50 m, 50-100 m, 100-150 m, 150-200 m, 200-250 m, 250-300 m, and >300 m (Figure 10e). The distribution of landslide area showed that 46.16% of the total landslide area was concentrated in the distance to rivers class of <50 m, as shown in Table 2.

Land use

The land use map of the research location was prepared using Google Earth Engine analysis and supported by the Indonesia Topographic Map of Gunungkidul and Klaten Regencies from Geospatial Information Agency (2014). Land use in the research location is grouped into six classes: settlement, rice field, orchard, shrubland, grassland, and agricultural field (Figure 10f). The distribution of landslide area showed that 93.06% of the total landslide area was concentrated in the land use class of agricultural fields, as shown in Table 2.

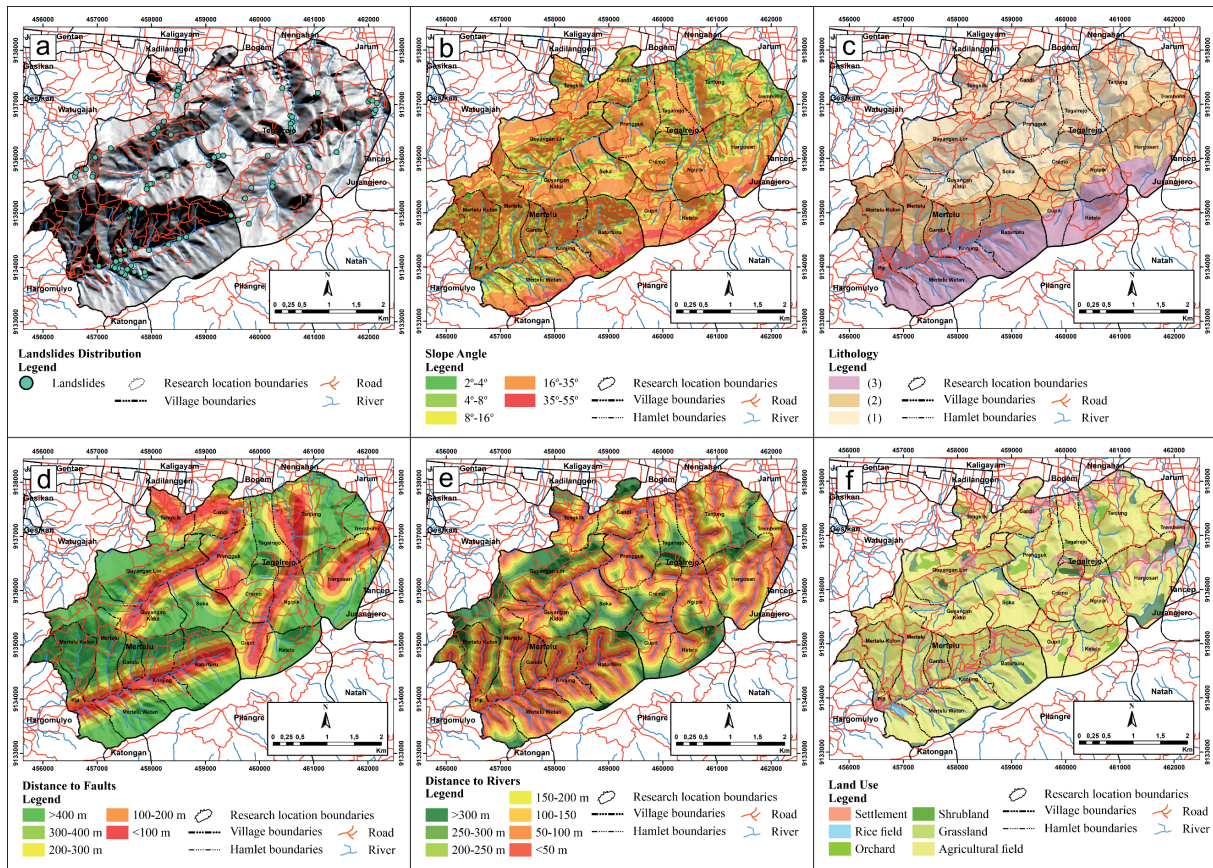


Figure 10. (a) Landslide distribution map, (b) Slope angle map, (c) Lithology map, (d) Distance to fault map, (e) Distance to rivers map, and (f) Land use map

Landslide susceptibility zoning using the WoE method

The first step to producing a landslide susceptibility map is dividing the dataset into a training dataset and a test dataset. A total of 73 landslide data, 58 data (80%) from the entire landslide data are allocated for the training dataset, while the remaining 15 data (20%) are allocated for the test dataset. The accuracy of the map was calculated using the area under curve (AUC) method, including the success rate curve (SRC) and prediction rate curve (PRC).

The weight of each parameter class was obtained by calculating the density of landslides in the training dataset within each parameter class. The positive and negative weights of each parameter class were calculated based on Equations 1 and 2. Then, the value of the contrast weight for each parameter class is obtained by calculating the difference between the positive weight and the negative weight, as shown in Equation 3. The result of the weighting class parameter using the WoE method can be observed in Table 3.

Table 3. The parameters used in the analyses and results of Weight of Evidence

Parameter	x	z	c	a	y	b	W+	W-	Cw
Slope Angle									
2°-4°	0.00	6,247.25	19,182,998.76	618,562.02	6,247.25	18,564,436.73	0.0000	0.0328	-0.0328
4°-8°	0.00	6,247.25	19,182,998.76	1,927,434.89	6,247.25	17,255,563.86	0.0000	0.1059	-0.1059
8°-16°	2,056.75	6,247.25	19,182,998.76	6,278,355.23	4,190.5	12,904,643.52	0.0059	-0.0029	0.0088
16°-35°	4,190.50	6,247.25	19,182,998.76	9,743,764.61	2,056.75	9,439,234.15	0.2781	-0.4019	0.6799
35°-55°	0.00	6,247.25	19,182,998.76	614,881.99	6,247.25	18,568,116.76	0.0000	0.0326	-0.0326

Parameter	x	z	c	a	y	b	W+	W-	Cw
Lithology									
(1)	1,599.25	6,247.25	19,182,998.76	7,731,819.68	4,648	11,451,179.07	-0.4539	0.2202	-0.6742
(2)	3,038.75	6,247.25	19,182,998.76	6,430,797.10	3,208.5	12,752,201.65	0.3722	-0.2580	0.6302
(3)	1,609.25	6,247.25	19,182,998.76	5,020,381.97	4,638	14,162,616.78	-0.0159	0.0056	-0.0214
Distance to Faults									
<100 m	3,504.25	6,247.25	19,182,998.76	2,794,515.46	2,743	16,388,483.30	1.3482	-0.6656	2.0138
100-200 m	1,081.50	6,247.25	19,182,998.76	2,937,925.80	5,165.75	16,245,072.95	0.1225	-0.0239	0.1464
200-300 m	645.50	6,247.25	19,182,998.76	2,981,972.31	5,601.75	16,201,026.45	-0.4084	0.0599	-0.4683
300-400 m	84.00	6,247.25	19,182,998.76	2,883,443.67	6,163.25	16,299,555.09	-2.4140	0.1493	-2.5634
>400 m	932.00	6,247.25	19,182,998.76	7,585,141.52	5,315.25	11,597,857.23	-0.9747	0.3416	-1.3164
Distance to Rivers									
<50 m	2,883.75	6,247.25	19,182,998.76	4,078,118.55	3,363.5	15,104,880.21	0.7753	-0.3802	1.1555
50-100 m	1,341.5	6,247.25	19,182,998.76	3,702,571.26	4,905.75	15,480,427.49	0.1066	-0.0273	0.1339
100-150 m	719.25	6,247.25	19,182,998.76	3,127,308.35	5,528	16,055,690.40	-0.3478	0.0556	-0.4035
150-200 m	408	6,247.25	19,182,998.76	2,551,117.25	5,839.25	16,631,881.51	-0.7111	0.0752	-0.7863
200-250 m	454.5	6,247.25	19,182,998.76	2,018,728.02	5,792.75	17,164,270.73	-0.3691	0.0357	-0.4048
250-300 m	0.00	6,247.25	19,182,998.76	1,481,428.58	6,247.25	17,701,570.17	0.0000	0.0804	-0.0804
>300 m	440.25	6,247.25	19,182,998.76	2,223,726.74	5,807	16,959,272.01	-0.4977	0.0501	-0.5478
Land Use									
Settlement	292.50	6,247.25	19,182,998.76	2,233,512.57	5,954.75	16,949,486.19	-0.9110	0.0758	-0.9868
Rice field	0.00	6,247.25	19,182,998.76	112,321.89	6,247.25	19,070,676.86	0.0000	0.0059	-0.0059
Orchard	0.00	6,247.25	19,182,998.76	479,862.54	6,247.25	18,703,136.22	0.0000	0.0253	-0.0253
Shrubland	141.00	6,247.25	19,182,998.76	597,286.92	6,106.25	18,585,711.83	-0.3218	0.0088	-0.3306
Grassland	0.00	6,247.25	19,182,998.76	69,926.67	6,247.25	19,113,072.08	0.0000	0.0037	-0.0037
Agricultural Field	5,813.75	6,247.25	19,182,998.76	15,690,088.16	433.5	3,492,910.59	0.1291	-0.9647	1.0938

The LSI of the landslide susceptibility zone map based on Equation 4 ranges from -5.116 to 5.573. The LSI value then reclassified into four landslide susceptibility classes based on BSN (National Standardization Agency of Indonesia) classification: very low (-5.116 - -2.292) covering 6.34% of the total research area, low (-2.292 - -0.539) covering 24.15% of the total research area, moderate (-0.539 - 1.419) covering 44.46% of the total research area, and high (1.419 - 5.573) covering 25.05% of the total research area (Figure 11).

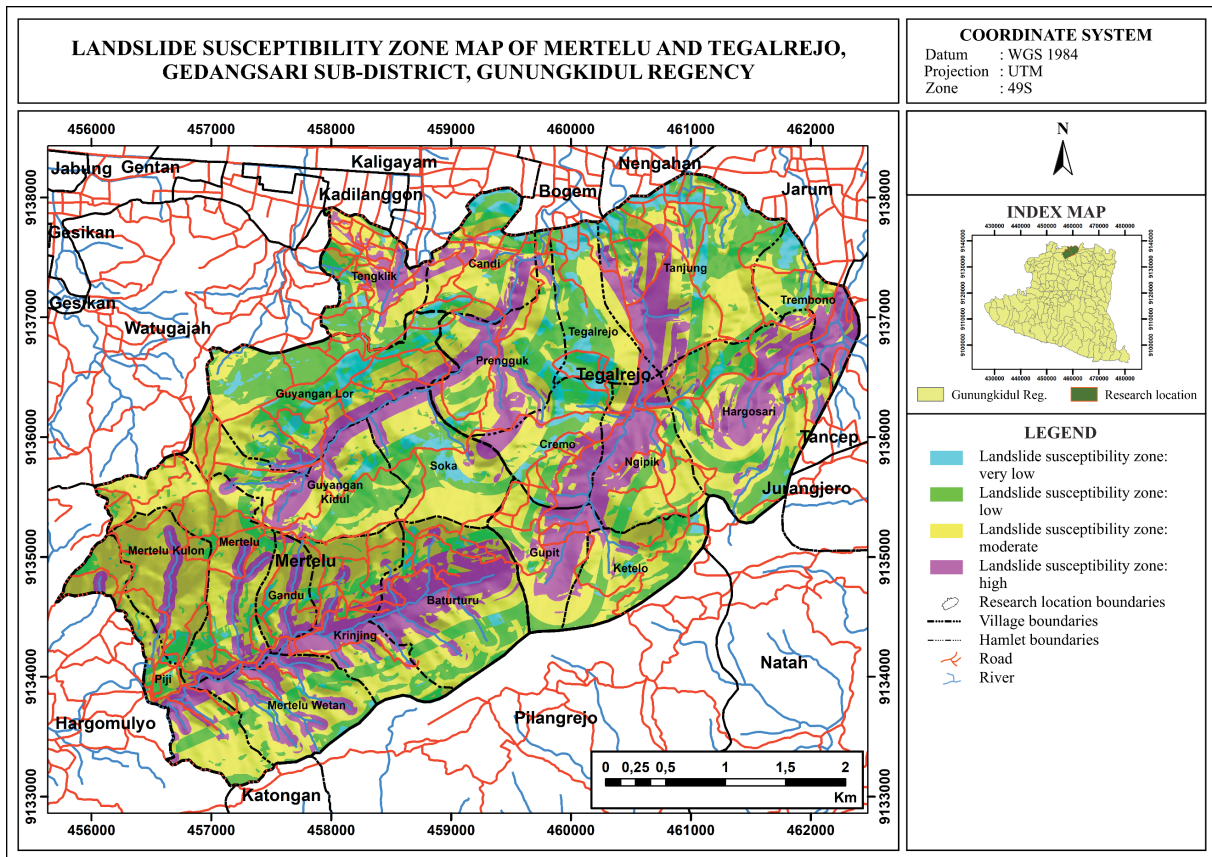


Figure 11. Landslide susceptibility zone map of Mertelu and Tegalrejo using WoE method

In general, the research location is classified into a medium to high landslide susceptibility zone, covering 69.51% of the total research area. Based on Table 3 and Figure 11, it is revealed that medium to high susceptibility zones are areas with distances close to faults and rivers. The distance to faults class of <100 m has the highest contrast weight value, followed by the distance to rivers class of <50 m, which also has a high contrast weight value. These high contrast weight values indicate that these class parameters respectively contribute toward landslide occurrences in the research location (e.g. Cellek, 2023; Kumar & Anbalagan, 2019).

VALIDATION

The validation of the model is an important step to assess its accuracy. Several approaches were used to evaluate the accuracy of the landslide susceptibility map, but the most commonly used are the success rate curve (SRC) and prediction rate curve (PRC). SRC and PRC can be obtained by initially grouping the LSI into ten equal-area classes (Pradhan et al., 2010). Then, the curve is produced by comparing the cumulative percentage of landslide area occurrences in each class with the cumulative percentage of area for each class (Ilia & Tsangaratos, 2016). SRC uses the cumulative percentage of landslide area from the training dataset, while PRC uses the cumulative percentage of landslide area from the test dataset. The curve that has been generated is then measured for its area to obtain the area under the curve value (AUC).

The AUC calculation results that the SRC value is 0.753 and the PRC value is 0.780 (Figure 12). Both values indicate that the landslide susceptibility map of this study has a good performance. Interestingly, the PRC value in this research shows better results than the SRC value. These results are also commonly found in other similar studies, such as the research conducted by Affandi et al. (2023), Grabowski et al. (2022), and Gupta et al. (2022). These results are due to the training dataset consisting of more landslides with larger areas compared to the landslides in the test dataset (Grabowski et al., 2022).

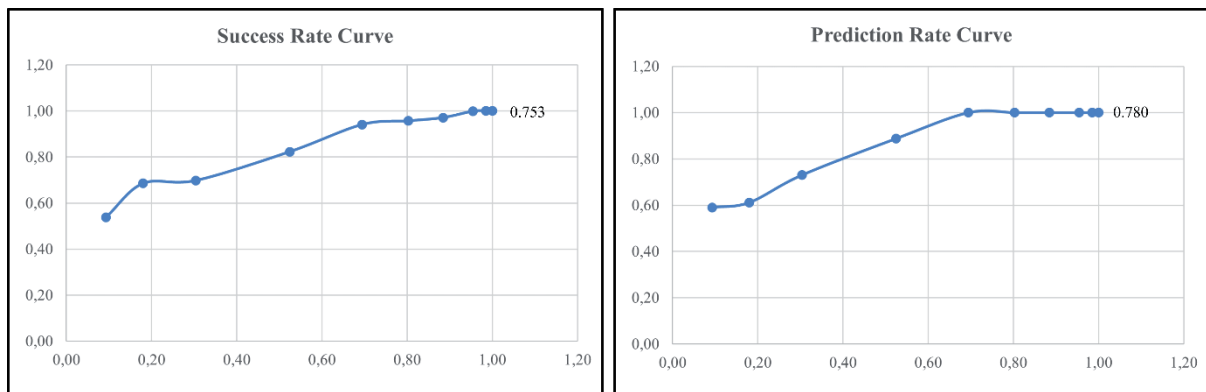


Figure 12. The success rate AUC value (left) and prediction rate AUC (right) of landslide susceptibility map using the WoE Method.

CONCLUSION

This research used the WoE method to identify and analyze the landslide susceptibility zone in Mertelu and Tegalrejo, Gedangsari sub-district, Gunungkidul Regency, Special Region of Yogyakarta. Based on the result of this research, Mertelu and Tegalrejo are classified into four landslide susceptibility zones, i.e., very low with 6.34% covering the area, low with 24.15% covering the area, moderate with 44.46% covering the area, and high with 25.05% covering the area. The landslide susceptibility map shows that the research location is predominantly characterized by areas with medium to high susceptibility to landslides. The medium and high susceptibility zones are close to the rivers that serve as the alignment of the faults. Additionally, these zones are located in areas with steep slope angles, composed of lithological units of tuffaceous sandstone with siltstone, breccia, and tuff intercalations, or interbedded tuffaceous sandstone-lapilli tuff with tuff intercalations, also predominantly consist of agricultural field. The obtained AUC values of SRC and PRC are 0.753 and 0.780. Both values indicate that the landslide susceptibility maps of this research have a good performance and are acceptable. According to the landslide susceptibility map in Mertelu and Tegalrejo, further research for the study area is important regarding landslide mitigation, settlement area, and land use planning and development from geological perspectives.

ACKNOWLEDGMENTS

The authors acknowledge the government of Gedangsari Sub-district, Gunungkidul Regency for their support during our site investigation and mapping. This research was funded by the Department of Geological Engineering, Faculty of Engineering, Universitas Gadjah Mada, through the scheme of 'Hibah Penelitian Dosen Tahun 2023 Departemen Teknik Geologi, Fakultas Teknik UGM'.

REFERENCES

- Affandi, E., Ng, T.F., Pereira, J.J., Ahmad, F., & Banks, V.J. (2023). Revalidation Technique on Landslide Susceptibility Modelling: An Approach to Local Level Disaster Risk Management in Kuala Lumpur, Malaysia. *Applied Sciences*, 13 (2), 768. <https://doi.org/10.3390/app13020768>.
- Bacha, A. S., Shafique, M., & van der Werf, H. (2018). Landslide inventory and susceptibility modelling using geospatial tools, in Hunza-Nagar valley, northern Pakistan. *Journal of Mountain Science*, 15(6), 1354–1370. <https://doi.org/10.1007/s11629-017-4697-0>
- Bariato, D. H., Margono, U., Husein, S., Novian, M. I., & Permana, A. K. (2017). Peta Geologi Lembar Wonosari (1408-31). *Pusat Survei Geologi Badan Geologi Kementerian Energi Dan Sumber Daya Mineral*.
- Bekkar, M., Djemma, H. K., & Alitouche, T. A. (2013). Evaluation Measures for Models Assessment over imbalanced data sets. *Journal of Information Engineering and Applications*, 3(10), 27–38. <https://doi.org/10.7176/JIEA>
- Blais-Stevens, A., Behnia, P., Kremer, M., Page, A., Kung, R., & Bonham Carter, G. (2012). Landslide susceptibility mapping of the Sea to Sky transportation corridor, British Columbia, Canada: comparison of two methods. *Bulletin of Engineering Geology and the Environment*, 71, 447–466. <https://doi.org/10.1007/s10064-012-0421-z>

- Budianta, W. (2020). Pemetaan Kawasan Rawan Tanah Longsor di Kecamatan Gedangsari, Kabupaten Gunungkidul, Yogyakarta dengan Metode Analytical Hierarchy Process (AHP). *Jurnal Pengabdian Kepada Masyarakat*, 6, 68–73. <https://doi.org/10.22146/jpkm.45637>
- Cellek, S. (2023). Linear Parameters Causing Landslides: A Case Study of Distance to the Road, Fault, and Drainage. *Kocaeli Journal of Science and Engineering*, 6(2), 94–113. <https://doi.org/10.34088/kojose.1117817>
- Dahal, R. K., Hasegawa, S., Nonomura, A., Yamanaka, M., Masuda, T., & Nishino, K. (2008). GIS-based weights-of-evidence modelling of rainfall-induced landslides in small catchments for landslide susceptibility mapping. *Environmental Geology*, 54, 311–324. <https://doi.org/10.1007/s00254-007-0818-3>
- Dai, F. C., Lee, C. F., & Zhang, X. H. (2001). GIS-based geo-environmental evaluation for urban land-use planning: a case study. *Engineering Geology*, 61, 257–271. [https://doi.org/10.1016/S0013-7952\(01\)00028-X](https://doi.org/10.1016/S0013-7952(01)00028-X)
- Das, J., Saha, P., Mitra, R., Alam, A., & Kamruzzaman, M. (2023). GIS-based data-driven bivariate statistical models for landslide susceptibility prediction in Upper Tista Basin, India. *Heliyon*, 9(5), e16186. <https://doi.org/10.1016/j.heliyon.2023.e16186>
- Getachew, N., & Meten, M. (2001). Weights of Evidence Modeling for Landslide Susceptibility Mapping of Kabi-Gebro Locality, Gundomeskel Area, Central Ethiopia. *Geoenvironmental Disasters*, 8(6). <https://doi.org/10.1186/s40677-021-00177-z>
- Grabowski, D., Laskowicz, I., Małka, A., & Rubinkiewicz, J. (2022). Geoenvironmental Conditioning of Landsliding in River Valleys of Lowland Regions and Its Significance in Landslide Susceptibility Assessment: A Case Study in the Lower Vistula Valley, Northern Poland. *Geomorphology*, 419, 108490. <https://doi.org/10.1016/j.geomorph.2022.108490>
- Gupta, V., Kumar, S., Kaur, R., and Tandon, R.S. (2022). Regional-Scale Landslide Susceptibility Assessment for the Hilly State of Uttarakhand, NW Himalaya, India. *Journal of Earth System Science*, 131(1), 2. <https://doi.org/10.1007/s12040-021-01746-4>
- Hungr, O., Leroueil, S., & Picarelli, L. (2014). The Varnes classification of landslide types, an update. *Landslides*, 11, 167–194. <https://doi.org/10.1007/s10346-013-0436-y>
- Ilija, I., & Tsangaratos, P. (2016). Applying Weight of Evidence Method and Sensitivity Analysis to Produce a Landslide Susceptibility Map. *Landslides*, 13, 379–397. <https://doi.org/10.1007/s10346-015-0576-3>
- Karnawati, D. (2007). Mekanisme Gerakan Massa Batuan Akibat Gempabumi: Tinjauan dan Analisis Geologi Teknik. *Dinamika Teknik Sipil*, 7, 179–190. <http://hdl.handle.net/11617/125>
- Kumar, R., & Anbalagan, R. (2019). Landslide susceptibility mapping of the Tehri reservoir rim area using the weights of evidence method. *Journal of Earth System Science*, 128, 153. <https://doi.org/10.1007/s12040-019-1159-9>
- Li, L., & Lan, H. (2023). Bivariate landslide susceptibility analysis: clarification, optimization, open software, and preliminary comparison. *Remote Sensing*, 15(5), 1418. <https://doi.org/10.3390/rs15051418>
- Pamela, Sadisun, I. A., Kartiko, R. D., & Arifianti, Y. (2018). Metode Kombinasi Weight of Evidence (WoE) dan Logistic Regression (LR) untuk Pemetaan Kerentanan Gerakan Tanah di Takengon, Aceh. *Jurnal Lingkungan Dan Bencana Geologi*, 9(2), 77–86. <https://jlbgeologi.esdm.go.id/index.php/jlbge>
- Pradhan, B., Oh, H. J., & Buchroithner, M. (2010). Weight of Evidence Model Applied to Landslide Susceptibility Mapping in a Tropical Hilly Area. *Geomatics, Natural Hazard and Risk*, 1(3), 199–223. <https://doi.org/10.1080/19475705.2010.498151>
- Prasetyadi, C., Sudarno, I., Indranadi, V. B., & Surono. (2011). Pola dan Genesa Struktur Geologi Pegunungan Selatan, Provinsi Daerah Istimewa Yogyakarta dan Provinsi Jawa Tengah. *Jurnal Sumber Daya Geologi*, 21, 91–107. <https://doi.org/10.33332/jgsm.geologi.v21i2.138>
- PVMBG. (2013). Peta Zona Kerentanan Gerakan Tanah Kabupaten Gunungkidul, D. I. Yogyakarta. *Pusat Vulkanologi Dan Mitigasi Bencana Geologi*.
- Shirzadi, A., Chapi, K., Shahabi, H., Solaimani, K., Kaviani, A., & Bin Ahmad, B. (2017). Rock fall susceptibility assessment along a mountainous road: an evaluation of bivariate statistic, analytical hierarchy process and frequency ratio. *Environmental Earth Sciences*, 76, 152. <https://doi.org/10.1007/s12665-017-6471-6>
- Surono. (2009). Litostratigrafi Pegunungan Selatan Bagian Timur Daerah Istimewa Yogyakarta dan Jawa Tengah. *Jurnal Sumber Daya Geologi*, 19(3), 209–221. <https://doi.org/10.33332/jgsm.geologi.v19i3.206>
- van Westen, C. J., Castellanos, E., & Kuriakose, S. L. (2008). Spatial data for landslide susceptibility, hazard, and vulnerability assessment: An overview. *Engineering Geology*, 102(3–4), 112–131. <https://doi.org/10.1016/j.enggeo.2008.03.010>
- van Zuidam, R. A. (1985). *Aerial Photo-Interpretation in Terrain Analysis and Geomorphic Mapping*. International Institute for Aerospace Survey and Earth Science (ITC) 978-9070043247.
- Yalcin, A., & Bulut, F. (2007). Landslide susceptibility mapping using GIS and digital photogrammetric techniques: a case study from Ardesen (NE-Turkey). *Natural Hazards*, 41, 201–226. <https://doi.org/10.1007/s11069-006-9030-0>
- Yatini, Y., & Suyanto, I. (2018). Identification of slip surface based on geoelectrical dipole-dipole in the landslides hazardous area of Gedangsari District, Gunungkidul Regency, Province of Daerah Istimewa Yogyakarta, Indonesia. *IOP Conf. Ser.: Earth Environ. Sci.* 212, 012013. <https://doi.org/10.1088/1755-1315/212/1/012013>